Augmenting Robot-Assisted Pattern-Cutting With Periodic Perturbations: Can We Make Dry Lab Training More Realistic?

Yarden Sharon, Tifferet Nevo, Daniel Naftalovich, Lidor Bahar, Yael Refaely, and Ilana Nisky, *Senior Member, IEEE*

Abstract*—*Objective: **Teleoperated robot-assisted minimally-invasive surgery (RAMIS) offers many advantages over open surgery, but RAMIS training still requires optimization. Existing motor learning theories could improve RAMIS training. However, there is a gap between current knowledge based on simple movements and training approaches required for the more complicated work of RAMIS surgeons. Here, we studied how surgeons cope with time-dependent perturbations. *Methods:* We used the da Vinci Research Kit and investigated the effect of time-dependent force and motion perturbations on learning a circular pattern-cutting surgical task. Fifty-four participants were assigned to two experiments, with two groups for each: a control group trained without perturbations and an experimental group trained with 1 Hz perturbations. In the first experiment, force perturbations alternatingly pushed participants' hands inwards and outwards in the radial direction. In the second experiment, the perturbation constituted a periodic up-and-down motion of the task platform. *Results:* Participants trained with perturbations learned how to overcome them and improve their performances during training without impairing them after the perturbations were removed. Moreover, training with motion perturbations provided participants with an advantage when encountering the same or other perturbations after training, compared to training without perturbations. *Conclusion:* Periodic perturbations can enhance RAMIS training without impeding the learning of the perturbed task. *Significance:* Our results demonstrate that using challenging training tasks that include perturbations can better prepare surgical trainees for the dynamic environment they will face with patients in the operating room.**

***Index Terms*—Surgical skill acquisition, sensorimotor adaptation, human-robot interaction, surgical robotics.**

Manuscript received 8 November 2023; revised 15 February 2024 and 5 June 2024; accepted 15 August 2024. Date of publication 27 August 2024; date of current version 16 January 2025. The work of Yarden Sharon was supported by the Besor scholarship and the Israeli Planning and Budgeting Committee scholarship. This work was supported in part by Helmsley Charitable Trust through the Agricultural, Biological and Cognitive Robotics Initiative and the Marcus Endowment Fund, both at Ben-Gurion University of the Negev, and in part by the ISF under Grant 327/20. *(Corresponding author: Yarden Sharon.)*

Yarden Sharon is with the Department of Biomedical Engineering, Ben-Gurion University of the Negev, Beer-Sheva 8410501, Israel, also with the Zelman Center for Brain Science Research, Ben-Gurion University of the Negev, Beer-Sheva 8410501, Israel, and also with the Haptic Intelligence Department, Max Planck Institute for Intelligent Systems, 70569 Stuttgart, Germany (e-mail: shayar@post.bgu.ac.il).

Tifferet Nevo, Lidor Bahar, and Ilana Nisky are with the Department of Biomedical Engineering, Ben-Gurion University of the Negev, Israel, and also with the Zelman Center for Brain Science Research, Ben-Gurion University of the Negev, Israel.

Daniel Naftalovich is with the Department of Computational & Mathematical Sciences, California Institute of Technology, USA, and also with the Keck School of Medicine of USC, University of Southern California, USA.

Yael Refaely is with the Thoracic Surgery Unit, Soroka Medical Center, Israel.

This article has supplementary downloadable material available at https://doi.org/10.1109/TBME.2024.3450702, provided by the authors.

Digital Object Identifier 10.1109/TBME.2024.3450702

I. Introduction

IN ROBOT-ASSISTED minimally-invasive surgery (RAMIS), surgeons use robotic manipulators to control the movements of instruments inserted into the patient's body via small incisions [1]. RAMIS offers many advantages over open surgery [2], but to benefit from them, surgeons must be well-trained [3]. Many efforts have been invested in optimizing the way RAMIS surgeons acquire technical skills [4], [5], [6], [7], [8], [9], [10], [11], but how to best train RAMIS surgeons is still unknown.

Insights concerning how to train RAMIS surgeons can be gained from motor learning studies [12] aiming to identify the different processes that enable learning. These studies define two essential concepts: skill acquisition is an improvement in performance beyond previous levels or the acquisition of entirely novel abilities [13], and adaptation is an improvement in performance in response to altered conditions, such as to perturbing force fields [14]. Both types of learning are important for surgical skill acquisition, but due to the gap between current motor learning knowledge based on simple movements and the complex motor tasks that RAMIS surgeons need to perform, it is not known whether combining the two types of learning in a single protocol can benefit training. Moreover, motor learning studies show that using perturbations that impair performance during training can enhance motor learning and improve performance after the perturbations are removed [15]. Several studies have investigated the effect of such perturbations on RAMIS training [16]. For example, the results of [17] suggest that training with forces that amplify the error may positively affect performance

improvement. However, more work is needed to test whether perturbations can be used to develop efficient training protocols.

One of the knowledge gaps between motor learning and surgical training is how surgeons cope with time-dependent perturbations. In fact, surgeons may encounter time-dependent perturbations during surgery. Factors that can contribute to these perturbations include the heartbeat, the pulsation of blood vessels, and the breathing movements of the patient. In these scenarios, it is crucial that surgeons' actions consider these perturbations to prevent damage to the tissue. Surgeons report that with experience, they adapt to working in the presence of such perturbations. However, motor learning studies suggest that participants do not adapt to time-varying perturbations [18]. To design training programs that can optimally prepare trainees to work in the presence of human body movement, it is important to study the effect of time-dependent perturbations on learning surgical tasks.

Training programs for RAMIS include dry and wet lab training [19], [20], [21]. In dry lab training, trainees perform tasks such as pattern-cutting, knot-tying, and suturing on inanimate mechanical models [22], [23]. In wet lab training, trainees can practice on frozen animal parts, frozen human body parts, anesthetized animals, or cadavers [20], [23]. Most wet labs use frozen animal parts because of their relatively lower costs [20]. However, when using frozen parts, similar to dry lab training, trainees do not face the challenges of bodily movements. To prepare for this challenge, several physical body motion simulators have been developed over the years [24], [25], [26], [27], [28]. However, how these time-dependent motion perturbations affect the motor learning of the surgeons is not understood.

There are several ways in which the motor system can cope with time-dependent perturbations. One example is to adapt by adjusting the internal model and applying opposing forces (e.g., forces in anticipation of the heart rate) to compensate for the perturbations. In this case, an after-effect could occur after the removal of the perturbations, which may be expressed as hand fluctuations at the rate of the removed perturbations. Such fluctuations may affect a surgeon's performance during the transition from an environment with organ movements to one without. A second way to tackle perturbations is increasing arm stiffness, which may contribute to stability and improve performance even in environments without organ movements or other perturbations. A third alternative is to change the task's temporal coordination to match the perturbations' tempo. Each way has different implications for the surgeon's performance and training. Therefore, understanding how surgeons cope with time-dependent perturbations is essential for designing better training approaches.

This experimental study is the first to examine the effect of time-dependent perturbations on learning a dry-lab surgical training task. We conducted two experiments in which the participants were required to cut circles drawn on a planar piece of gauze. In the first experiment, participants were subjected to perturbations that alternately pushed their hands inwards and outwards in the radial direction. This type of perturbation simulates a situation in which forces are applied to the surgeon's hand by a surgical tool in contact with a moving tissue. It happens in procedures such as off-pump cardiac surgery when operating on the heart or in thoracic surgery during dissection and suturing of large blood vessels. These forces are caused by tissue motion and are encountered in both open and thoracoscopic surgeries and robotic platforms with force feedback. While in a realistic situation, surgeons are not facing forces continuously pushing their hand in a radial direction, we chose this perturbation because it maximizes the error between the desired path and the actual path in our planar dry-lab task. Thus, it may properly model how surgeons cope with time-dependent force perturbations. In the second experiment, simulating a more realistic situation, the perturbations occurred as the task platform's up-and-down periodic motion. We hypothesized that trainees would reduce errors with training. This hypothesis was confirmed. We subsequently tested whether this learning leads to an after-effect impairing the ability of the surgical trainees to cope with other conditions (such as an environment without perturbations) and whether it improves their resistance to other subsequent perturbations.

The experiments addressed four questions:

- **Q1** – Can participants improve their performance under periodic perturbations?
- **Q2** – Does training with periodic perturbations impair the performance when the perturbations are removed?
- **Q3** – Can training with periodic perturbations improve performance when later encountering the same perturbations, compared to training without perturbations?
- **Q4** – Can training with periodic perturbations improve performance when encountering different perturbations, compared to training without perturbations?

A pilot version of this study with 10 participants in the experiment with force perturbations was summarized in [29].

II. Methods

A. The da Vinci Research Kit (dVRK)

The dVRK is a RAMIS research platform [30] provided by Intuitive Surgical (Sunnyvale, CA). Its hardware consists of components from the first-generation da Vinci Surgical System [31]. Our dVRK (Fig. 1) consists of a pair of Master Tool Manipulators (MTMs), a pair of Patient Side Manipulators (PSMs), a foot-pedal tray, a stereo viewer, and four manipulator interface boards. In this study, the participants sat on the master side (Fig. 1(b)) and used the MTMs to teleoperate curved scissors and a large needle driver on the patient side where the task board was placed (Fig. 1(c)). The MTMs' and PSMs' electronics were connected via firewire to a single Ubuntu (UNIX) OS computer with an Intel Xeon E5-2630 v3 processor. The vision system consisted of a pair of Blackfly S cameras (FLIR Integrated Imaging Solutions Inc.) fixed so that the task board was in the center of the field of view. The participants could not control the cameras or the zoom. The video was broadcast using custom-developed software on a dedicated computer to the stereo viewer, which presented a 3D view at a 35 Hz refresh rate with a 1080×810 resolution per eye. The movement scaling was set to 0.4 so that each movement of the PSM was 0.4 times the movement of the

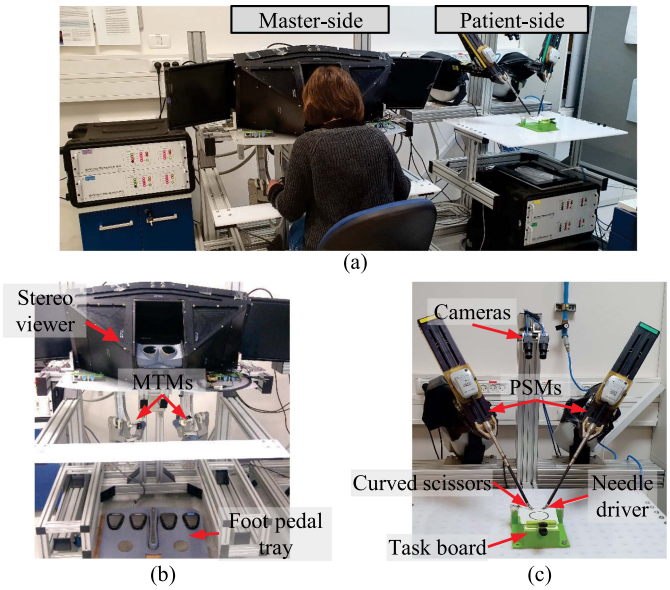

Fig. 1. The dVRK. (a) The participant sits on the master side and uses the MTMs to remotely teleoperate the PSMs on the patient side. (b) The master side. (c) The patient side.

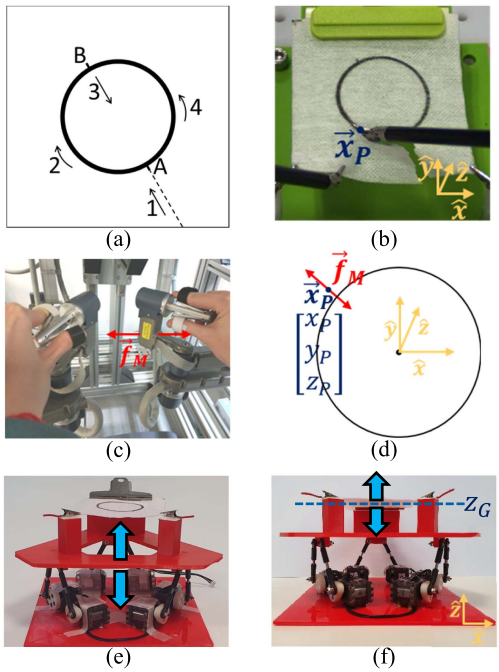

Fig. 2. The pattern-cutting task and the two types of perturbations. (a) The task sequence. (b) The task board and the two PSM tools (right – curved scissors, left – large needle driver). (c) The MTMs and the force applied in Experiment 1. (d) The circle, the position of the right PSM's tip $\vec{x}_P$ (blue), the force applied on the participant's hand $\vec{f}_M$ (red) in Experiment 1, and the reference base frame (yellow). (e) The moving platform in Experiment 2. (f) The z position of the gauze Z_G (blue) in Experiment 2.

MTM, and the participants could reach the entire workspace without using the foot pedal.

B. The Pattern-Cutting Task

The task performed during this study's experiments was a modified FLS pattern-cutting task [32]. Participants used their right hand to control curved scissors and cut a 5 cm diameter circle (line width 2 mm) drawn on a two-layered 10 × 10 cm non-woven gauze. To complete the task, they could cut both layers or one layer (if the bottom layer became separated from the top layer). The task sequence consisted of (Fig. 2(a), (b)): (1) cutting the gauze towards point A; (2) cutting along the left half of the circle until point B; (3) moving the scissors back to point A; (4) cutting the right side of the circle. The participants used their left hand to control a large needle driver and maintain the tension of the gauze. They were instructed to cut as quickly and accurately as possible (within the black line).

C. The Perturbations

This study consisted of two experiments, each consisting of different perturbations:

1) Experiment 1 - MTM's Force Perturbations: In some of this experiment's trials, planar radial force perturbations were applied to the participant's hand using the right MTM – towards and away from the center of the circle alternately (Fig. 2(c), (d)) – according to the following force, in Newtons:

$$\vec{f}_M = A(t)\left[\frac{x_P}{\sqrt{x_P^2+y_P^2}}, \frac{y_P}{\sqrt{x_P^2+y_P^2}}, 0\right]^T, \qquad (1)$$

where x_P and y_P are the x and y positions of the scissors' tip relative to the center of the circle, respectively (see Fig. 2(d)), and A(t) defines one of three types of trials (see Video 1):

- No perturbations: $A(t) = 0$.
- 1 Hz perturbations: $A(t) = \sin(2\pi t)$. We chose a maximal force of 1N in this trial, which was noticeable but still allowed task completion.
- Unpredictable perturbations: $A(t) = \frac{\sum_1^5 \sin(2\pi f t)}{\sqrt{5}}; f \sim U[0.3\text{ Hz}, 1\text{ Hz}]$. Such a combination of five sine waves is known to be unpredictable to human users [33]. We normalized the amplitude to equalize the power to the 1 Hz perturbations.

To ensure that the perturbations were in the radial direction, the gauze was placed so that the center of the circle was at the origin of the reference base frame (Fig. 2(d)). Before each trial, the PSM tool pointed to the origin of the reference base frame, and the experimenter placed the marked center of the circle at the marked position.

2) Experiment 2 - Environment Motion Perturbations: For this experiment, we manufactured a platform based on the Stewart Platform Research Kit (SPRK) design, a low-cost platform designed to simulate anatomical movements [27]. In our study, the platform moved up and down (Fig. 2(e), (f)). The z position of the gauze, Z_G, in centimeters, was defined according to the trial type (see Video 2):

- No perturbations: $Z_G = 0$.
- 1 Hz perturbations: $Z_G = 0.635 \cdot \sin(2\pi t)$. Here also, we chose the amplitude of the sine so that the movement was noticeable but still allowed task completion.
- Unpredictable perturbations: $Z_G = 0.568 \cdot \sum_1^5 \sin(2\pi f t); f \sim U[0.3\text{ Hz}, 1\text{ Hz}]$. The constant we used for

normalization is larger than in Experiment 1 because the movement of the platform was not noticeable with a smaller constant.

D. Experimental Protocol

Apart from the different perturbations – force or motion – the experimental protocol was the same for both experiments. Therefore, we describe the protocol of both experiments together. Notably, we did not combine different perturbation types in the same experiment; each participant was exposed to only one perturbation, i.e., force or motion, depending on the experiment in which he or she participated.

Thirty volunteers (aged 21–30) participated in Experiment 1 (force), and 24 volunteers (aged 22–29) participated in Experiment 2 (motion). All participants signed an informed consent approved by the Human Participants Research Committee of the Ben-Gurion University of the Negev (protocol number 1283-1, approved on 6.7.2015). To be included, volunteers had to be right-handed and without prior surgical training experience. We excluded surgeons because they encounter time-dependent perturbations daily, and we wished to minimize differences in prior exposure to such perturbations.

The participants were shown how to use the dVRK and perform the pattern-cutting task. Since the perturbations of Experiment 1 (force) were based on the circle's position, the importance of keeping the gauze in place was emphasized, i.e., it should not be pulled in a way that distorts the marked circle. The instructions were accompanied by videos of the pattern-cutting task, showing correct performance and an incorrect performance in which the participant stretched the gauze in a prohibited way and did not cut within the black line. Before the experiment, each participant practiced the following actions with the robot: pressing the right pedal to start teleoperation, moving the right tool through the task sequence (without cutting), holding the gauze with the left tool, and cutting a straight line with the right tool.

For each of the two experiments, the participants were randomly assigned into two groups: an *experimental* group ($N_{Exp.1\ (force)}$=15, $N_{Exp.2\ (motion)}$=12) and a *control* group ($N_{Exp.1\ (force)}$=15, $N_{Exp.2\ (motion)}$=12). During the experiment, they performed 24 consecutive trials (see Fig. 3). Note that the type of perturbations described below are according to the experiment (Experiment 1- force or Experiment 2 - motion):

- **Baseline (B)** – 5 trials without perturbations. These trials were the same for both groups in both experiments, and their purpose was to assess the baseline performance of each participant.
- **Training (T)** – 10 trials addressing Q1: the *control* groups trained without perturbations, and the *experimental* groups trained with 1 Hz perturbations.
- **Post-training (P)** – 9 trials testing the effect of the training on post-training performance, i.e., addressing Q2-Q4; these trials were the same for both groups in each experiment. The first three trials **(P1)** were without perturbations and assessed the performance of both groups after the different training protocols (Q2). The next three trials **(P2)** were with 1 Hz perturbations and assessed the resistance to 1 Hz perturbations (Q3). The last three trials **(P3)** were with unpredictable perturbations and aimed to assess the resistance to new perturbations participants had not encountered before (Q4). The five frequencies of the unpredictable trials varied between the three trials but were the same for all participants in each experiment.

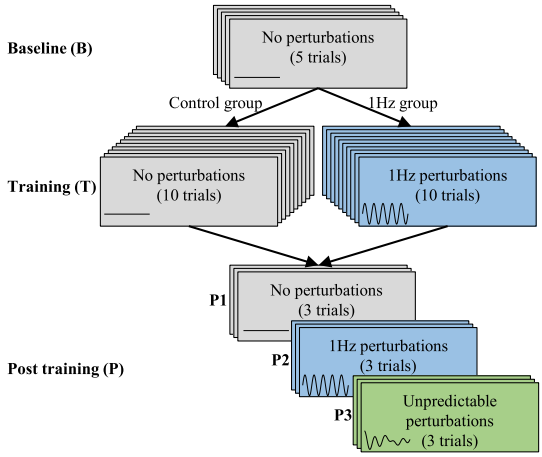

Fig. 3. The experimental protocol.

According to this protocol, the *experimental* groups were exposed to both no-perturbations and perturbations trials. In contrast, the *control* groups were only exposed to the no-perturbations trials during the baseline and training trials. This choice was critical for addressing participant variability in the baseline performance and obtaining a meaningful comparison between the groups. The number of trials per stage was selected based on a pilot experiment [29] showing that some metrics varied greatly between trials, but after 10 training trials, most participants reached a plateau in performance.

E. Data Acquisition and Prepossessing

All the kinematic data of the MTMs and PSMs were recorded at 100 Hz. To avoid errors resulting from small variations in the sampling intervals, we interpolated the PSMs position data to 100 Hz using piecewise cubic Hermite interpolating polynomial (PCHIP). The video data of the left camera were recorded at 35 Hz, and all cut circles were scanned. We used the recorded videos and the scissors' opening angle to manually segment each trial into its stages. All raw data are available for download at [34].

Technical issues in some trials resulted in trial termination before task completion. Participants completed the task after the issue was fixed, but the trials were removed from the analysis. In Experiment 1 (force), 20 out of the 720 trials were removed, and in Experiment 2 (motion), 22 out of 576 were removed. When fewer than two trials were left for a participant at a certain stage, we removed the entire stage from the analysis. This occurred in stage **P3** of Experiment 2 (motion) for one participant from the control group and one from the experimental group.

Extracting the height of the moving platform $\mathbf{z_G(t)}$ *for trials with 1 Hz perturbations (Fig. 4):* We initially directly measured

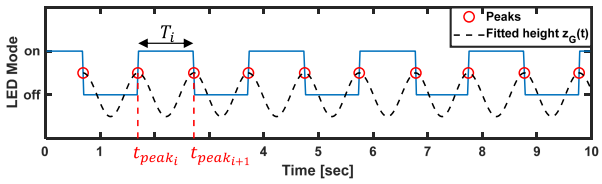

Fig. 4. Extracting the height of the moving platform $z_G(t)$.

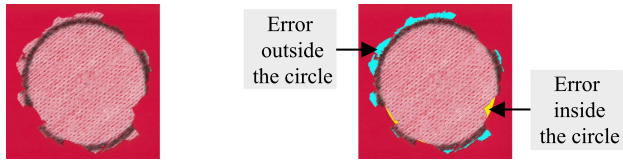

Fig. 5. Example of the total error calculation: (a) The cut circle. (b) The circle with marked error zones.

the height of the moving platform through communication with the controller. However, when we tested its movement, we discovered that continuously sending the data from the controller creates delays in the movement of the platform. Therefore, we used the alternative method using the LED mode of the controller. We programmed the moving platform controller so that the LED indicator switched mode (on/off) every time the platform reached the peak height. We obtained the LED mode at each frame via image processing using the videos recorded during each trial. We defined the platform's peak heights using the timestamps where the LED switched its mode. To calculate the height of the moving platform between peaks, we first calculated the time period of each cycle as:

$$T_i = t_{peak_{i+1}} - t_{peak_i}, \tag{2}$$

where t_{peak_i} and $t_{peak_{i+1}}$ are the peak times at the beginning and end of the ith cycle, respectively. Then, the height values for the ith cycle were fitted using:

$$FittedCycle_i(t) = \cos\left(\theta_i(t)\right), \text{ where:}$$
$$\theta_i(t) = \frac{2\pi}{T_i}\left(t - t_{peak_i}\right) \tag{3}$$

The complete signal of the moving platform height, $z_G(t)$, was achieved by concatenating all the fitted cosine cycles.

F. Metrics

We used four metrics to assess the participants' progress: *combined error-time*, *path length*, *1 Hz tool movement*, and *cutting phase* (for Experiment 2 - motion). The first two metrics quantified the task performance, and the other two enabled the investigation of the different approaches of the participants.

1) Combined Error-Time: Participants were instructed to cut as quickly and accurately as possible. According to the speed-accuracy trade-off [35], we expected that shorter task times might be accompanied by larger errors and vice versa. Hence, we combined these two performance measures. The task time was calculated as follows:

$$TT = t_{end} - t_{start}, \tag{4}$$

where t_{start} is the time when the participant first closes one of the tools on the gauze, and t_{end} is the time of the last cut when the circle had been completely removed from the gauze.

To quantify the errors, we used a custom-written image processing algorithm written in MATLAB that detected error zones in the scanned circles, defined as areas where the cutting was not performed on the line, i.e., outside or inside the circle (Fig. 5(a), (b)). The total error was:

$$TE = E_{\text{outside}} + E_{\text{inside}}, \tag{5}$$

where $E_{outside}$ and E_{inside} are the numbers of pixels in the error zones outside and inside the circle, respectively.

The combined error-time of trial j was calculated as [36]:

$$CET_j = \frac{TT_j - \overline{TT}}{S_{TT}} + \frac{TE_j - \overline{TE}}{S_{TE}}, \tag{6}$$

where $\overline{TT}$ and $\overline{TE}$ are the average values of the task times and the total errors across all trials conducted by all participants in the experiment (calculated separately for Experiment 1 and Experiment 2), and S_{TT} and S_{TE} are the respective standard deviations. Note that the value of this metric can be positive or negative, where lower values imply better performance. Participants are expected to complete the task faster and more accurately with practice; therefore, this metric's value is expected to decrease during training.

2) Path Length: This metric is a common measure of surgical skill quantifying the economy of motion, calculated as:

$$PL = \sum_{n=1}^{N-1} ||\vec{\boldsymbol{x}}_P[n+1] - \vec{\boldsymbol{x}}_P[n]||_2, \tag{7}$$

where $\vec{\boldsymbol{x}}_P[i]$ is the scissors' tip position at the ith sample, and N is the number of samples. Participants are expected to improve their economy of motion, and therefore, the value of this metric is expected to decrease during training.

3) 1 Hz Tool Movement: This metric quantifies the effect of the perturbations on the participant's movement. The higher the value of this metric, the greater the 1 Hz fluctuations in the hand movement. To detect such movement in the scissors, we used spectral analysis to calculate the amplitude of the 1 Hz component of the tool's movement. We used the same spectral analysis for both experiments but analyzed a different signal in each experiment.

In Experiment 1 (force), we analyzed the planar radial component of the scissors' path (Fig. 6(a)):

$$r_{xy_P}[n] = \sqrt{x_P[n]^2 + y_P[n]^2}, \tag{8}$$

where x_P and y_P are the x and y position coordinates of the scissors' tip. The size of the fluctuations in the radial direction is a measure for coping with the perturbations, either by adaptation – i.e., actively canceling the perturbation with opposing forces, or by increasing the arm stiffness. Participants who apply

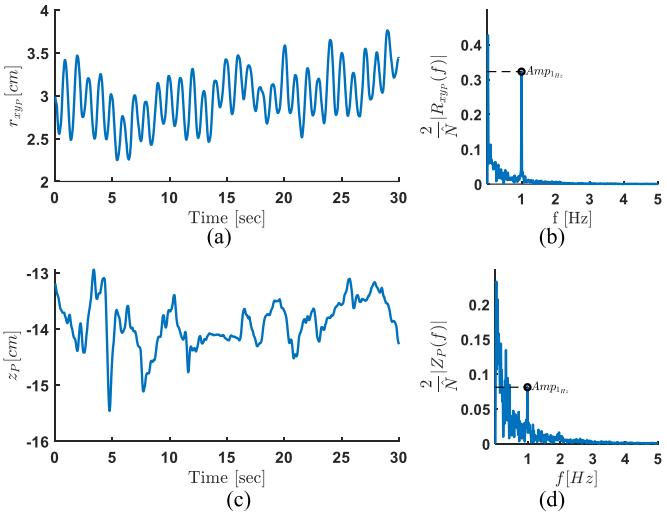

Fig. 6. Example of the 1 Hz tool movement metric. (a) An example from Experiment 1 (force): the planar radial component of the scissors' path. (b) The Fourier transform of the planar radial component of the scissors' path. The amplitude in 1 Hz is marked. (c) An example from Experiment 2 (motion): the vertical component of the scissors' path. (d) The Fourier transform of the vertical component of the scissors' path. The amplitude in 1 Hz is marked.

an opposing force that is similar in magnitude and opposite in direction to the perturbing force or higher arm stiffness decrease the size of the fluctuation in their hand movement. Therefore, the more the participant actively cancels the perturbation, the value of this metric is expected to decrease during training.

In Experiment 2 (motion), we analyzed the vertical component of the scissors' path, $z_P[n]$ (Fig. 6(c)). A possible approach to dealing with the perturbations in this experiment is to follow the movement of the platform and move the scissors up and down with the platform. Such movement would increase the value of this metric.

We will denote the analyzed signal by $g[n]$: for Experiment 1 (force) $g[n] = r_{xy_P}[n]$, and for Experiment 2 (motion) $g[n] = z_P[n]$. First, to avoid spectral leakage and allow appropriate resolution for detecting of 1 Hz frequency, we shortened the length of the signals by rounding it down to $\hat{N}$, the nearest multiple of 100:

$$\hat{N} = floor(N, 100). \tag{9}$$

Second, we calculated the discrete Fourier transform (DFT) of the signal:

$$G[k] = \sum_{n=1}^{\hat{N}} (g[n] - \overline{g}) e^{-j\frac{2\pi}{\hat{N}}(k-1)(n-1)}, \quad 1 \le k \le \hat{N}, \tag{10}$$

where $\overline{g}$ is the average of $g[n]$. Then, we found all the k values corresponding to the range of 1 ± 0.015 Hz:

$$f[k] = f_s \frac{k-1}{\hat{N}} = 100\frac{k-1}{\hat{N}}[Hz]$$
$$\mathbf{k}_{1_{Hz}} = \{k : 0.985 \le f[k] \le 1.015\} \tag{11}$$

where f_s is the sampling frequency. Lastly, the amplitude of the 1 Hz component was defined using the maximum of $|G[k]|$ within this range:

$$Amp_{1_{Hz}} = \frac{2}{\hat{N}} \cdot \max\{|G[\mathbf{k}_{1_{Hz}}]|\}. \tag{12}$$

We normalized by $\frac{2}{\hat{N}}$ so that if $g[n]$ is a 1 Hz sinusoidal wave with an amplitude A, we will obtain $Amp_{1_{Hz}} = A$.

Fig. 6(b) and (d) show examples of Fourier transforms for the analyzed signals, and the $Amp_{1_{Hz}}$ for each signal.

In Experiment 1 (force), the perturbations were designed to increase the error only while cutting the circle. Therefore, we calculated $Amp_{1_{Hz}}$ for steps 2 and 4 (Fig. 2(a)) and averaged them to obtain one metric value per trial.

4) Cutting Phase: In Experiment 2 (motion), another approach to dealing with the perturbations was timing the cuts to the minima and the maxima of the sinusoidal movement of the platform, as suggested in [37]. To investigate the timing strategies of the participants, we calculated the values of the cosine phase θ (3) when the participants performed cuts. To find the cuts, we used the MATLAB function `findpeaks()` to find the local minima of the recorded scissors' opening angle. Two examples of the cutting phases are presented in Fig. 7. For participants who time their cuts to a particular phase of the movement, we expect to find more frequent cuts around this preferred phase.

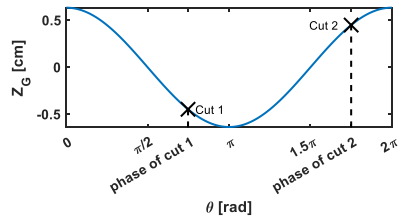

Fig. 7. Calculating the cutting phase. The figure shows the z position of the gauze, Z_G, as a function of the phase θ for one cycle of the moving platform. Two example cuts are marked with a black x, and their phases are shown on the horizontal axis.

G. Statistical Analysis

1) Research Questions Q1-Q4: Since our metrics were not normally distributed, we tested our hypotheses using permutation tests [38]. In order to compare the different stages using the same number of trials, we calculated the average metric values for each participant as follows: the last three trials of the baseline (B), the first three trials of the training (T_{start}), the last three trials of the training (T_{end}), the post-training trials without perturbations ($P1$), the post-training trials with 1 Hz perturbations ($P2$), and the post-training trials with unpredictable perturbations ($P3$).

We first tested Q1 – can participants improve their performance under periodic perturbations? For each metric, we calculated the difference between T_{start} and T_{end} of each participant. We then used a matched-pair permutation test for each group to test whether the mean of the differences significantly differed from zero. Additionally, we used a permutation test to examine whether the means of the individual differences between T_{start}

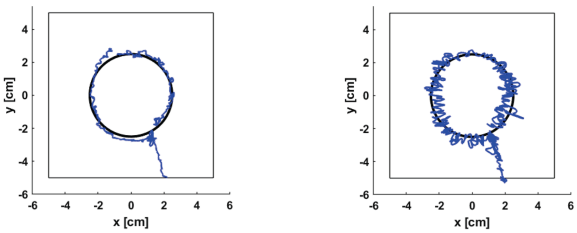

Fig. 8. Examples of the recorded path of the scissors. (a) The last baseline trial without perturbations. (b) The same participant's first training trial with 1 Hz perturbations.

and T_{end} were significantly different between the two groups (*control* and *experimental*). We then tested Q2 – does training with periodic perturbations impair the performance when the perturbations are removed? We performed a permutation test to examine whether there was a significant difference between the mean $P1$ values of the two groups. In addition, we calculated the improvement between the baseline and the P1 trials ($B - P1$, subtracting $P1$ from B) and used the outcome for another permutation test between the two groups. Next, we tested Q3 – can training with periodic perturbations improve performance when later encountering the same perturbations, compared to training without perturbations? We performed two permutation tests between the groups: (1) $P2$ values and (2) $P2 - P1$ values. Lastly, we tested Q4 – can training with periodic perturbations improve performance when encountering different perturbations, compared to training without perturbations? We performed two permutation tests between the groups: (1) $P3$ values and (2) $P3 - P1$ values.

For each experiment and research question, we adjusted the p values according to the Holm-Bonferroni correction for multiple comparisons [39]. Statistical significance was determined at the 0.05 threshold. We used the MATLAB Statistics Toolbox for our analysis.

2) Timing of the Cuts: We tested whether participants in the *experimental* group of Experiment 2 (motion) timed their cuts to a specific phase of sinusoidal movement of the platform. We obtained the *cutting phase* values from all their trials with 1 Hz perturbations – ten training trials and three $P2$ trials. We performed a chi-squared test for each participant with the null hypothesis that the cutting phases are distributed uniformly, i.e., there is no preferred cutting phase.

III. Results

Fig. 8 shows the scissors' path when a participant in Experiment 1 (force) cut the circle. The deviations from the circle in Fig. 8(b) are more prominent than those in Fig. 8(a), demonstrating that the force perturbations affected the scissors' path. Fig. 9 shows the values of the three metrics during the trials. Fig. 10 presents the average values for the different experiment stages (left panels) and the average values of the individual differences between the stages (right panels). Videos 1 and 2 present the trials with the lowest and highest scores for each metric.

For both Experiment 1 (force) and Experiment 2 (motion), there were no significant differences between the two groups at the baseline stage (Exp. 1: $p_{\text{combined error-time}} = 0.2160$, $p_{\text{path length}} = 0.9985$, $p_{\text{radial 1 Hz movement}} = 0.9695$; Exp. 2: $p_{\text{combined error-time}} = 0.8625$, $p_{\text{path length}} = 0.4755$, $p_{\text{vertical 1 Hz movement}} = 0.6260$). In the following subsections, we will present the results of our tests, summarised in Tables I and II.

A. Q1 – The Effect of the Training Protocols on the Learning Curves and Approaches

In both experiments, participants from both groups improved their *combined error-time* scores with statistical significance during training. In Experiment 1 (force), both groups improved their *path length* scores with statistical significance during training. In addition, the average *path length* improvement of the *experimental* group was significantly higher than the same improvement for the *control* group. Because the perturbations in this experiment directly increase the path length, the improvement of the *experimental* group probably comprises both an improvement as a result of learning the task (similar to the *control* group) and an additional improvement caused by tackling the perturbations.

Participants from the *experimental* groups of both experiments significantly reduced their *1 Hz tool movement* scores during training. This means that at the end of the training, the 1 Hz fluctuations in their movement were smaller than at the beginning.

B. Q2 – The Effect of the Training Protocols on Post-Training Trials Without Perturbations (P1)

After training (P1), the groups reached similar performance levels in terms of *combined error-time* and *path length*. In addition, within each experiment, no significant difference between the values of *1 Hz tool movement* of the *experimental* and *control* groups was observed. These results suggest that there is no after-effect, and that training with perturbations did not impair performance after they were removed.

C. Q3 and Q4 – The Effect of the Training Protocols on Post-Training Trials With 1 Hz Perturbations (P2), and the Effect of the Training Protocols on Post-Training Trials With Unpredictable Perturbations (P3)

In Experiment 2 (motion), for the *combined error-time* and *path length* scores, the individual differences between trials with 1 Hz perturbations (P2) and trials without perturbation after training (P1) significantly differed between the *experimental* and *control* groups. A larger difference between the two groups was observed for the individual differences between trials with unpredictable perturbations (P3) and trials without perturbation after training (P1). These results suggest that training with motion perturbations provided the *experimental* group with an advantage over the *control* group, both when encountering the same perturbations as they trained with and when encountering new perturbations.

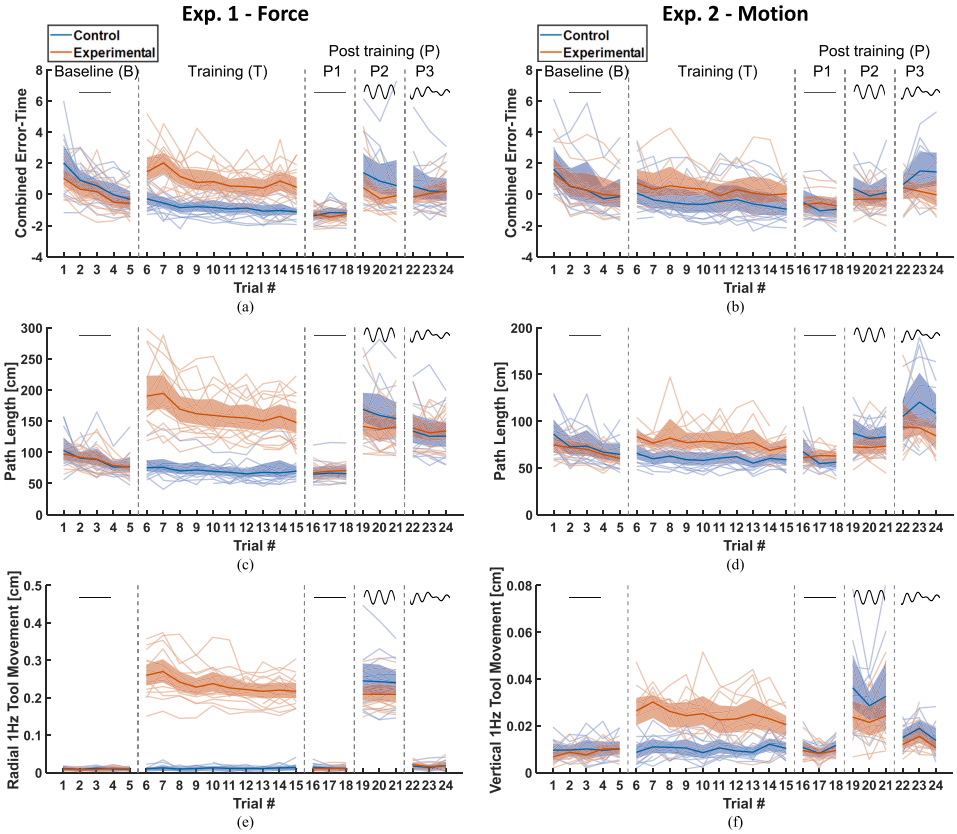

Fig. 9. The values of the three metrics for each trial. Each light-colored line represents a participant, dark colors are the participants' means, and the shaded areas represent the 95% bootstrap confidence intervals.

TABLE I
STATISTICAL ANALYSIS SUMMARY – EXPERIMENT 1 (FORCE)

	Q1			Q2		Q3		Q4	
	Training start – training end (T_{start}–T_{end})			Post no pert. (P1)	Baseline –post no pert. (B–P1)	Post 1Hz (P2)	Post 1Hz –post no pert. (P2–P1)	Post unpred. (P3)	Post unpred. –post no pert. (P3–P1)
	Control	Exp.	Exp.– Control	Exp.– Control	Exp.– Control	Exp.– Control	Exp.– Control	Exp.– Control	Exp.– Control
Combined error-time	Δ=0.515 p=0.002	Δ=0.963 p=0.002	Δ=0.448 p=0.07	Δ=-0.08 p=0.591	Δ=-0.325 p=0.337	Δ=-0.835 p=0.202	Δ=-0.772 p=0.202	Δ=-0.207 p=1	Δ=-0.126 p=1
Path length	Δ=5.627 p=0.012	Δ=32.778 p<0.001	Δ=27.151 p<0.001	Δ=3.531 p=0.899	Δ=-3.508 p=0.899	Δ=-21.81 p=0.133	Δ=-25.341 p=0.115	Δ=7.845 p=1	Δ=4.314 p=1
Radial 1Hz movement	Δ=-0.001 p=0.181	Δ=0.039 p=0.001	Δ=0.041 p<0.001	Δ=-0.001 p=1	Δ=0.001 p=1	Δ=-0.033 p=0.229	Δ=-0.032 p=0.229	Δ=0.002 p=0.465	Δ=0.003 p=0.398

Exp. is an abbreviation for *experimental*. The symbol "–" denotes subtraction. The symbol "Δ" denotes the mean of the individual differences for matched-pair tests and the difference between the means of the two groups for the other tests. Results highlighted in gray indicate statistically significant effects ($p < 0.05$).

TABLE II
STATISTICAL ANALYSIS SUMMARY – EXPERIMENT 2 (MOTION)

	Q1			Q2		Q3		Q4	
	Training start – training end (T_{start}–T_{end})			Post no pert. (P1)	Baseline –post no pert. (B–P1)	Post 1Hz (P2)	Post 1Hz –post no pert. (P2–P1)	Post unpred. (P3)	Post unpred. –post no pert. (P3–P1)
	Control	Exp.	Exp.– Control	Exp.– Control	Exp.– Control	Exp.– Control	Exp.– Control	Exp.– Control	Exp.– Control
Combined error-time	Δ=0.493 p=0.013	Δ=0.534 p=0.036	Δ=0.042 p=0.881	Δ=0.132 p=1	Δ=0.006 p=1	Δ=-0.44 p=0.264	Δ=-0.572 p=0.011	Δ=-1.004 p=0.041	Δ=-1.014 p=0.03
Path length	Δ=4.197 p=0.131	Δ=7.048 p=0.131	Δ=2.852 p=0.427	Δ=2.439 p=0.491	Δ=-5.965 p=0.156	Δ=-12.039 p=0.054	Δ=-14.478 p=0.016	Δ=-20.038 p=0.061	Δ=-23.468 p=0.018
Vertical 1Hz movement	Δ<0.001 p=0.724	Δ=0.004 p=0.021	Δ=0.004 p=0.052	Δ=-0.001 p=0.462	Δ=0.001 p=0.64	Δ=-0.01 p=0.134	Δ=-0.008 p=0.134	Δ=-0.002 p=0.316	Δ=-0.001 p=0.49

Exp. is an abbreviation for *experimental*. The symbol "–" denotes subtraction. The symbol "Δ" denotes the mean of the individual differences for matched-pair tests and the difference between the means of the two groups for the other tests. Results highlighted in gray indicate statistically significant effects ($p < 0.05$).

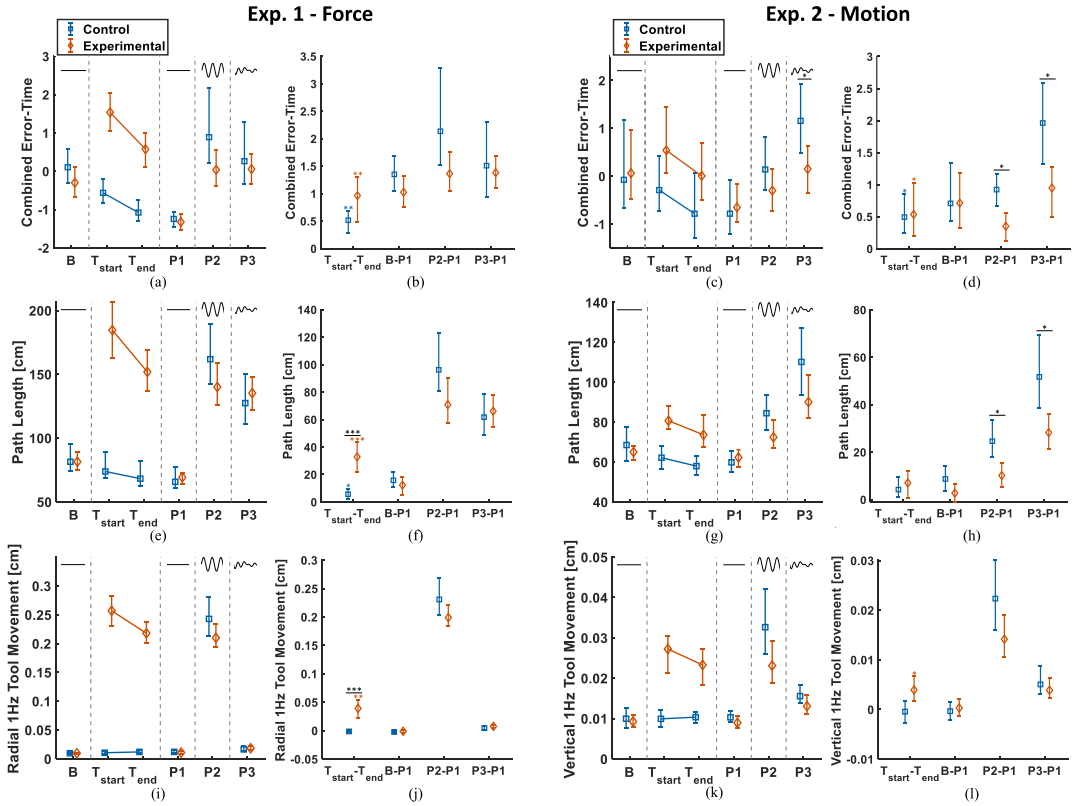

Fig. 10. The left panel of each experiment presents the average values of the three metrics at the different experiment stages: the last three baseline trials (B), first three training trials (T_{start}), last three training trials (T_{end}), post-training trials without perturbations (P1), post-training trials with 1 Hz perturbations (P2), and the post-training trials with unpredictable perturbations (P3). The right panel of each experiment presents the average values of the individual differences between the stages: T_{start}–T_{end}, B–P1, P2–P1, P3–P1. The markers are the means, and the error bars are 95% bootstrap confidence intervals. The full report of all the tests is presented in Tables I and II. Values that were statistically significant are indicated with asterisks, according to: $^{*}p < 0.05$, $^{**}p < 0.01$, and $^{***}p < 0.001$.

D. Timing of the Cuts

The chi-squared tests showed that for 3 out of 12 participants in the *experimental* group of Experiment 2 (motion), the cuts' phases distribution was not uniformly distributed. Only 3 participants timed their cuts to specific phases of the sinusoidal movement. Accordingly, most participants (9 out of 12) did not employ a strategy of timing the gauze cutting to a specific phase of the platform movement. Fig. 11 presents examples of the cuts' phase distributions.

IV. Discussion

We tested the effect of periodic time-dependent perturbations on learning a RAMIS training task. We found that participants who trained with force or motion periodic perturbations improved at the same rate as the control participants who trained without perturbations. After the training, when the perturbations were removed, their performances were similar regardless of training type. Hence, learning to deal with perturbations did not undermine the ability to learn to perform the task better, and trainees could train in challenging conditions without impairing their learning. Importantly, we found that training with perturbations provided these participants with an advantage over training without perturbations when they encountered the same or new perturbations (albeit the latter only in the case of motion perturbations, which simulate organ movement). In addition, we aimed to gain insights into potential learning mechanisms that enable these improvements in the presence of perturbations. Our results ruled out learning through an adaptation mechanism involving building an internal representation of the perturbations and were compatible with other possible mechanisms that enable improving performances during training with perturbations.

It is known that practice makes perfect, but how to design an effective practice is still an open question. Previous studies have shown that surgical performance could be improved by repetitions of dry lab tasks [10], [40]. However, dry lab training on static models does not prepare trainees to handle living tissue that may move during surgery. In this study, we show for the first time the positive effect of adding periodic perturbations to RAMIS training. The effect of forces depending on the error relative to a desired path has been previously investigated [16], [17], [41], but those studies focused on tasks in a static environment and did not deal with the challenges of more realistic dynamic environments. Hence, they could not provide us with insights about our study. Our findings propose a practical motivation for adding periodic perturbations to training – they prepare participants for dynamic environments they are likely to encounter in real-life procedures better than training under static conditions.

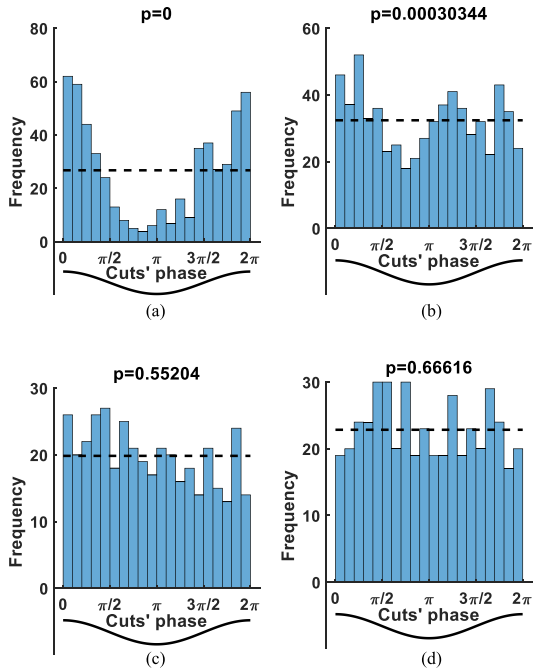

Fig. 11. Example of the cuts' phase histograms for participants in the *experimental* group of Experiment 2 (motion). The dashed horizontal black line indicates the expected frequency for uniformly distributed cuts. (a) and (b) The two participants with the lowest p-values. (c) and (d) The two participants with the highest p-values.

To design interventions for improving surgical training, it is crucial to understand the mechanisms that enable learning because different learning mechanisms and their interactions can affect the efficiency and quality of surgeons' performance improvement. For example, trainees may improve their performances in the presence of perturbations through an adaptation mechanism, in which the motor system adjusts the internal model that anticipates the outcomes of the motor commands [42]. However, adaptation leads to an after-effect when the perturbations are removed and may impair performances in the transition to a static environment.

We designed our experiments to test several possible coping mechanisms for time-dependent perturbations. Our findings that participants in both force and motion experiments improved their performance during training with 1 Hz periodic perturbations compared to their performance at the beginning of the training corroborate the anecdotal reports of practicing surgeons. Moreover, participants' *1 Hz tool movement* values decreased with training, indicating that the perturbations less affected their movements. Such a result could be due to adaptation, that is, improvement due to a change in motor commands due to building an internal representation of the perturbation [42]. In Experiment 1 (force), such adaptation would occur if the motor system learned the force perturbations and applied forces in the opposite direction to eliminate their effect. In Experiment 2 (motion), such adaptation would occur if the motor system learned the motion perturbations and moved the hand up and down with the platform to counteract the relative motion between the scissors and the platform. However, while adaptation results in after-effects, in our study, we did not find 1 Hz fluctuations in the trials without perturbation after training, and the *1 Hz tool movement* returned to the baseline level as soon as the perturbations were removed. We, therefore, conclude that adaptation did not occur. This is consistent with the results of studies of reaching movements in the presence of time-varying perturbations, suggesting that the sensorimotor system cannot adapt to time-dependent perturbations [18].

Although adaptation did not occur, the participants improved. Our results suggest that the mechanisms enabling this improvement are likely different for the two types of perturbations we examined. Previous studies have reported co-contraction of the muscles and an increase in the impedance of the arm in the face of unstable dynamics [43]; this phenomenon could be behind the decrease in *1 Hz tool movement* with training observed in Experiment 1 (force). In this experiment, the perturbations directly pushed the hand and increased the error between the desired path (the circle) and the actual path. Increasing the impedance of the arm and decreasing the size of the fluctuations in the movement could lead to improved performance in the pattern-cutting task without after-effects. Therefore, based on our results, we suggest the increase in the impedance of the arm as one of the mechanisms that could enable coping with dynamic environments.

In Experiment 2 (motion), participants increased their 1 Hz vertical movement when the platform started moving at the beginning of the training. The perturbations in this experiment were the platform movement, which did not act directly on the participant's hand. Therefore, an increase in *1 Hz tool movement* values had to result from an active movement of the participant's hand in response to the perturbations. During training with the motion perturbations, this 1 Hz hand movement decreased, and the performance of the participants improved. However, we cannot determine whether this 1 Hz movement helped perform the pattern-cutting task and whether it served as an immediate feedback mechanism replaced by a different coping mechanism. We tested another potential way of coping with the perturbations - timing the cuts to the minima and maxima of the platform movement. We found that most participants did not have a preferred phase of the sinusoidal movement for their cutting. To conclude this point, further research is required to explore the mechanisms that enable learning to cope with motion perturbations. Importantly, however, we found that the *experimental* group who trained with periodic 1 Hz motion perturbations performed better than the control group both in trials with 1 Hz perturbations and with unpredictable perturbations. Although we did not clearly identify the mechanisms that enabled the improvement of the *experimental* group, our results suggest that their learning was not specific to the 1 Hz motion perturbations because they could generalize this learning to cope with other motion perturbations.

Limitations and Future Work: Surgeons may encounter force perturbation during surgery when the tools are in contact with a moving tissue. This happens in open and thoracoscopic surgeries and in robotic platforms that enable force feedback. The perturbations in Experiment 1 (force) were less realistic since surgeons are not constantly in contact with moving tissue, and

the direction of the forces in surgery is not planar radial. However, as the first stage of testing coping mechanisms with periodic perturbations, it was important to use perturbations that would directly increase the error between the desired and the actual tool path. Moreover, using force perturbations that make the training more challenging by increasing the error may benefit the improvement of some trainees, even if they do not simulate real situations [17]. In our experiment, although the perturbation was designed to increase the error, we did not find that training with the periodic perturbing force improved the learning of the task (B-P1 values did not differ between the condition groups). Future studies can test whether using larger forces or different force directions may benefit the improvement of trainees. In addition, we found that an increase in the impedance of the arm could be one of the possible coping mechanisms with periodic force perturbations. It is important to note that increasing arm impedance can increase fatigue. Additionally, stabilizing the tool by increasing arm impedance can harm moving tissues since the tool will apply more force to the tissue. After our results shed some light on how participants cope with periodic force perturbations, future research should further examine the benefits and risks of training with these perturbations.

This study focused on isolating the effect of the perturbations on learning. Therefore, we invited participants without surgical knowledge and used a simple training task with an experimental setup that did not require moving the camera or using the clutch pedal. Future studies with participants with surgical knowledge and different expertise groups are needed, such as medical students, residents, fellows, and experienced surgeons. Moreover, studying a wider range of training tasks with an experimental setup similar to the clinical one will also shed additional light on ways to optimize RAMIS training.

V. Conclusion

In this study, we aimed to start bridging the gap between the fields of motor learning and RAMIS training. We designed an experiment to test the effect of adding force or motion periodic perturbations on learning the pattern-cutting task. We found that participants learned how to overcome the perturbations without impairing their performance after the perturbations were removed. Our results ruled out motor adaptation as the mechanism underlying this learning. Importantly, we found that training with motion (but not force) perturbations provided an advantage compared to training without perturbations, both for the perturbations participants trained with and other perturbations. Our results highlight the importance of designing challenging dry lab tasks that include motion perturbations to better prepare trainees for the dynamic environment they will face with patients in the operating room.

Acknowledgment

The authors thank Anton Deguet, Simon DiMaio, Eli Peretz, and Gilat Malka for their help with the dVRK integration, and Alon Lempert and Noa Yamin for running the experiments.

References

[1] S. Maeso et al., "Efficacy of the da vinci surgical system in abdominal surgery compared with that of laparoscopy: A systematic review and meta-analysis," *Ann. Surg.*, vol. 252, no. 2, pp. 254–262, Aug. 2010.
[2] K. Moorthy et al., "Dexterity enhancement with robotic surgery," *Surg. Endoscopy Other Interventional Techn.*, vol. 18, no. 5, pp. 790–795, May 2004.
[3] D. L. Crawford and A. M. Dwyer, "Evolution and literature review of robotic general surgery resident training 2002–2018," *Updates Surg.*, vol. 70, no. 3, pp. 363–368, Sep. 2018.
[4] S. Jacobs et al., "The impact of haptic learning in telemanipulator-assisted surgery," *Surg. Laparoscopy Endoscopy Percutaneous Techn.*, vol. 17, no. 5, Oct. 2007, Art. no. 402.
[5] K. Ahmed et al., "Development of a standardised training curriculum for robotic surgery: A consensus statement from an international multidisciplinary group of experts," *BJU Int.*, vol. 116, no. 1, pp. 93–101, Jul. 2015.
[6] K. Yang et al., "Effectiveness of an integrated video recording and replaying system in robotic surgical training," *Ann. Surg.*, vol. 265, no. 3, pp. 521–526, Mar. 2017.
[7] M. Shahbazi et al., "Multimodal sensorimotor integration for expert-in-the-loop telerobotic surgical training," *IEEE Trans. Robot.*, vol. 34, no. 6, pp. 1549–1564, Dec. 2018.
[8] A. E. Abdelaal et al., "Play me back: A unified training platform for robotic and laparoscopic surgery," *IEEE Robot. Automat. Lett.*, vol. 4, no. 2, pp. 554–561, Apr. 2019.
[9] P. M. S. Gurung et al., "Accelerated skills acquisition protocol (ASAP) in optimizing robotic surgical simulation training: A prospective randomized study," *World J. Urol.*, vol. 38, no. 7, pp. 1623–1630, Jul. 2020.
[10] R. M. Satava et al., "Proving the effectiveness of the fundamentals of robotic surgery (FRS) skills curriculum: A single-blinded, multispecialty, multi-institutional randomized control trial," *Ann. Surg.*, vol. 272, no. 2, pp. 384–392, Aug. 2020.
[11] S. Azadi et al., "Robotic surgery: The impact of simulation and other innovative platforms on performance and training," *J. Minimally Invasive Gynecol.*, vol. 28, no. 3, pp. 490–495, Mar. 2021.
[12] A. M. Jarc and I. Nisky, "Robot-assisted surgery: An emerging platform for human neuroscience research," *Front. Hum. Neurosci.*, vol. 9, Jun. 2015, Art. no. 315.
[13] J. W. Krakauer and P. Mazzoni, "Human sensorimotor learning: Adaptation, skill, and beyond," *Curr. Opin. Neurobiol.*, vol. 21, no. 4, pp. 636–644, Aug. 2011.
[14] R. Shadmehr and F. A. Mussa-Ivaldi, "Adaptive representation of dynamics during learning of a motor task," *J. Neurosci.*, vol. 14, no. 5, pp. 3208–3224, May 1994.
[15] J. Brookes et al., "Exploring disturbance as a force for good in motor learning," *PLos One*, vol. 15, no. 5, May 2020, Art. no. e0224055.
[16] M. M. Coad et al., "Training in divergent and convergent force fields during 6-DOF teleoperation with a robot-assisted surgical system," in *Proc. 2017 IEEE World Haptic. Conf.*, Jun. 2017, pp. 195–200.
[17] Y. A. Oquendo et al., "Haptic guidance and haptic error amplification in a virtual surgical robotic training environment," *IEEE Trans. Haptics*, early access, Jan. 05, 2024, doi: 10.1109/TOH.2024.3350128.
[18] A. Karniel and F. Mussa-Ivaldi, "Sequence, time, or state representation: How does the motor control system adapt to variable environments?," *Biol. Cybern.*, vol. 89, pp. 10–21, Aug. 2003.
[19] L. Jason et al., "Best practices for robotic surgery training and credentialing," *J. Urol.*, vol. 185, no. 4, pp. 1191–1197, Apr. 2011.
[20] A.N. Sridhar et al., "Training in Robotic Surgery—An overview," *Curr. Urol. Rep.*, vol. 18, no. 8, Jun. 2017, Art. no. 58.
[21] R. A. Fisher et al., "An over-view of robot assisted surgery curricula and the status of their validation," *Int. J. Surg.*, vol. 13, pp. 115–123, Jan. 2015.
[22] R. Smith, V. Patel, and R. Satava, "Fundamentals of robotic surgery: A course of basic robotic surgery skills based upon a 14-society consensus template of outcomes measures and curriculum development," *Int. J. Med. Robot. Comput. Assist. Surg.*, vol. 10, no. 3, pp. 379–384, Sep. 2014.
[23] L. Bresler et al., "Residency training in robotic surgery: The role of simulation," *Teach. Continuing Training Surg.*, vol. 157, no. 3, Supplement 2, pp. S123–S129, Jun. 2020.
[24] R. d. L. Stanbridge et al., "Use of a pulsatile beating heart model for training surgeons in beating heart surgery," *Heart Surg. Forum*, vol. 2, no. 4, pp. 300–304, Dec. 1999.
[25] O. Reuthebuch et al., "Advanced training model for beating heart coronary artery surgery: The Zurich heart-trainer," *Eur. J. Cardio-Thoracic Surg.*, vol. 22, no. 2, pp. 244–248, Aug. 2002.

[26] J. I. Fann et al., "Improvement in coronary anastomosis with cardiac surgery simulation," *J. Thoracic Cardiovasc. Surg.*, vol. 136, no. 6, pp. 1486–1491, Dec. 2008.
[27] V. Patel et al., "SPRK: A low-cost stewart platform for motion study in surgical robotics," in *Proc. IEEE 2018 Int. Symp. Med. Robot.*, Mar. 2018, pp. 1–6.
[28] S. Yasuda et al., "Implementation of a beating heart system for training in off-pump and minimally invasive coronary artery bypass," *BMC Surg.*, vol. 21, no. 1, Jan. 2021, Art. no. 26.
[29] Y. Sharon et al., "Preliminary analysis of learning a robot-assisted surgical pattern-cutting," in *Proc. Conf. New Technol. Computer/Robot Assist. Surg.*, Sep. 2020, pp. 94–95.
[30] P. Kazanzides et al., "An open-source research kit for the da vinci surgical system," in *Proc. 2014 IEEE Int. Conf. Robot. Automat.*, May 2014, pp. 6434–6439.
[31] G. S. Guthart and J. K. Salisbury, "The intuitive telesurgery system: Overview and application," in *Proc. IEEE Int. Conf. Robot. Automat.*, Apr. 2000, pp. 618–621.
[32] "FLS Manual Skills Written Instructions and Performance Guidelines," Feb. 2014. [Online]. Available: https://www.flsprogram.org/wp-content/uploads/2014/03/Revised-Manual-Skills-Guidelines-February-2014.pdf
[33] G. Avraham et al., "Toward perceiving robots as humans: Three handshake models face the turing-like handshake test," *IEEE Trans. Haptics*, vol. 5, no. 3, pp. 196–207, Apr. 2012.
[34] Y. Sharon, T. Nevo, D. Naftalovich, L. Bahar, Y. Refaely, and I. Nisky, "BGU pattern-cutting dataset (BGU-PatCut)," 2024, doi: 10.17617/3.JK4ANF.
[35] P. M. Fitts, "The information capacity of the human motor system in controlling the amplitude of movement," *J. Exp. Psychol.*, vol. 47, no. 6, pp. 381–391, Jun. 1954.
[36] H. R. Liesefeld and M. Janczyk, "Combining speed and accuracy to control for speed-accuracy trade-offs (?)," *Behav. Res. Methods*, vol. 51, no. 1, pp. 40–60, Feb. 2019.
[37] V. Patel et al., "Using intermittent synchronization to compensate for rhythmic body motion during autonomous surgical cutting and debridement," in *Proc. IEEE 2018 Int. Symp. Med. Robot.*, Mar. 2018, pp. 1–6.
[38] P. Good, *Permutation Tests: A Practical Guide to Resampling Methods for Testing Hypotheses*. Berlin, Germany: Springer, Apr. 2013.
[39] S. P. Wright, "Adjusted P-values for simultaneous inference," *Biometrics*, vol. 48, no. 4, pp. 1005–1013, Dec. 1992.
[40] I. Nisky et al., "Teleoperated versus open needle driving: Kinematic analysis of experienced surgeons and novice users," in *Proc. 2015 IEEE Int. Conf. Robot. Autom.*, May 2015, pp. 5371–5377.
[41] N. Enayati et al., "Robotic assistance-as-needed for enhanced visuomotor learning in surgical robotics training: An experimental study," in *Proc. 2018 IEEE Int. Conf. Robot. Automat.*, May 2018, pp. 6631–6636.
[42] R. Shadmehr, M. A. Smith, and J. W. Krakauer, "Error correction, sensory prediction, and adaptation in motor control," *Annu. Rev. Neurosci.*, vol. 33, no. 1, pp. 89–108, Jun. 2010.
[43] E. Burdet et al., "The central nervous system stabilizes unstable dynamics by learning optimal impedance," *Nature*, vol. 414, no. 6862, pp. 446–449, Nov. 2001.